Multiple prediction and reservoir characterization of a tight sand reservoir

Bo Zhao, ExxonMobil Exploration (formerly with dGB-USA), Friso Brouwer, dGB-USA, Fred Aminzadeh, dGB-USA, Stan Morris, Anadarko Petroleum, and Ron Harris, Anadarko Petroleum*

Summary

In reservoir property prediction, estimations of presence and thickness of reservoir are often found to be erroneous by drilling results. The reservoir in this study is onshore tight sand gas reservoir with a low impedance contrast between reservoir sands and encasing shale. In addition to the low amplitude of the reservoir reflector caused by the low-impedance contrast, multiple energy interferes with the primary reflector. This causes the reflector amplitudes to be decreased or enhanced. Subsequent predictions of thickness and porosity are unreliable as a result. In this study a number of methods are applied to minimize the effect of multiple interference and each method is validated against actual well measurements individually to assess its effectiveness. Secondly, attribute based Neural Network predictions are used to asses the impact of multiple contamination at a given point in order to predict where reservoir properties will be accurately predicted and where errors may occur.

Introduction

The study area is located onshore Texas. The depth of reservoir is approximately 17,000 ft. Ten wells were previously drilled with variable results. Seven wells were available for calibration, while and three wells were used as blind test.. The reservoirs show porosities in the range of 6-9%, with the sands in general having slightly higher impedances than the encasing shales. The amplitude strength of the reservoir reflection is strongly dependent on tuning (effects), with the sands being in tuning range for thicknesses between 80 and 200ft. However, low S/N ratios caused by low impedance contrast and the interfering multiple energy, make it difficult to distinguish between thicker and thinner reservoir sands using the full and partial stacks. However, on the gathers it is possible to correlate with good versus bad wells, indicating that the seismic contains sufficient information to discriminate between reservoir and non-reservoir. In this study a number of methods to improve reservoir property predictions were tested with well results (some of them blind test) as validation. First applied three methods of multiple recognition and removal (pattern recognition, Radon transform, and deconvolution) to improve thickness estimation based on amplitude and frequency characteristics of the reservoir reflector. The results of each method were validated against net sand thickness from the wells. Also evaluated was the use of acoustic impendence inversion as a means to a more stable prediction of reservoir properties in the presence of multiples. Secondly, we developed a set of attributes that potentially can highlight interference of multiples with the primary reflector. These attributes were combined using neural network technology and Support Vector Machine result in a multiple contamination map. This map can be used to assess the accuracy (confidence intervals) of the reservoir property predictions.

Synthetic seismic modeling and basic seismic attributes analysis

After detailed analysis of well logs, we made synthetic seismic models with the reflectivity of the well 1, which is representative for the seven wells available: higher impedance than above shale and blocky sand with thickness of 219 feet.

Although synthetic wedge models show a good relationship between amplitude and thickness (Figure 1), the crossplot of amplitude and thickness at the well locations (Figure 2) shows there are two outliers: the well 6 has a thickness of 38 feet, but amplitude of 55; the well 7 has a thickness of 164 feet, but amplitude of 38. These outliers may be attributed either to a irregular acquisition grid (Well 6) and/or multiple interference.

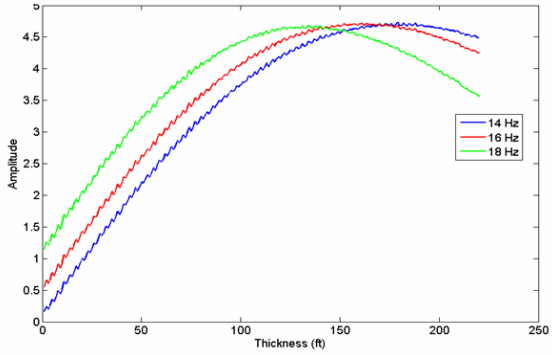

Figure 1. The relationship of Amplitude and instantaneous frequency against thickness.

Multiple prediction and reservoir characterization of a tight sand reservoir

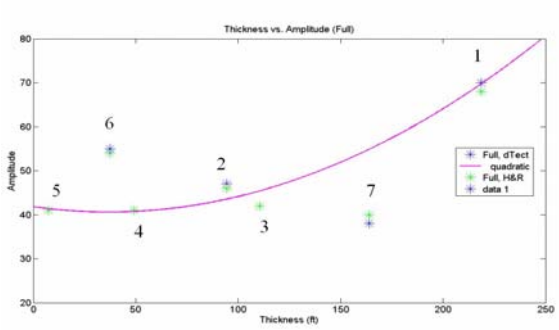

Figure 2. The crossplot of amplitude and thickness at the well locations. The blue dots are the amplitude values read from the full stack data in OpendTect. The green dots are the amplitude values read in Hampson-Russell. The magenta curve is quadratic fitting after taking out well 6 and well 7.

Acoustic Impedance inversion

In order to derive a better amplitude and thickness relationship, we inverted the acoustic impedance from the full stack seismic data. After testing three inversion options (bandlimited, model-based, and neural network) inversion, we found that on the cross section which has both of the wells 1 and Well 5, only neural network inversion distinguishes the thick well (Well 1) and the thin well (Well 5): neural network inversion picks the sand body at the reservoir level of 1 and this sand body disappears at the reservoir level of Well 5. Therefore, we chose neural network to invert the acoustic impedance. Why the neural network prediction has the best quality is not entirely clear, but it may be that the non-linear nature of neural networks is better capable of handling interferences in the signal due to the multiple interference.

To asses the robustness of the NN AI inversion we tested three variations in the original model building: First omitting Well 2, 4, and 5 from NN training; then omitting Well 6 and well 7 and in the third run omitting Well 1 and Well 3 from NN training.. Visually examining the match of inverted impedance and the impedance at the absent well locations for each variation, we found the neural network inversion which leaves out Well 1 and Well 3 in modeling matches best with the impedance at the absent well locations. The inversion results from these three variations have comparable correlation coefficients with the impedance of the input wells (from 0.75 to 0.79, see Table 1 inversion validation with cross-correlation). However, comparing with the first two variations, the third variation – leaving out Well 1 and Well 3 in original modeling – has a higher correlation coefficient (0.73) with the absent wells. Hence rotating the wells in and out the train set affects the result, implying the robustness of NN AI inversion is less than hoped for in this particular case.

Table 1. Inversion validation with cross-correlation

Inversion variations	Absent wells in modeling	Correlation with input wells	Correlation with absent wells
1	Well 2, Well 4 and Well 5	0.79	0.57
2	Well 6 and Well 7	0.77	0.59
3	Well 1 and Well 3	0.75	0.73

Multiple recognition

We tried two methods of multiple recognition that were based on seismic attributes. The methods were: pre-stack NN and post-stack NN. NN have the advantage that if there is no strong correlation between one input attribute and the target, (amount of multiple contamination) it can combine multiple attributes with weak correlations in a optimized prediction (Aminzadeh and de Groot, 2005)

For the pre-stack NN dip –in the time offset domain- and dip-related attributes are important in multiple recognition, since the data is NMO corrected and therefore dipping and non-aligned events will be indicators of multiple energy. Using dGB OpendTect software a steering cube was built for the whole gather volume (a steering cube is a 3D volume to guide the attribute calculation following the dip direction).. Other attributes that indicated multiple energy are frequency and irregular variations of maximum and minimum amplitude of an event with offset These attributes were calculated for the whole gather volume. Next we pick primary and multiple on the gathers. If one event is flat and continuous in the offset direction, we considered it as primary. If one event is dipping, we considered it as multiple. We attempted to make all the picks within the steering cube and made the picks evenly distributed along the whole gather cube. Based on these manually picked example points we trained the NN to classify the gathers into primary and multiple and applied it to the whole gather volume. (see attachment for Neural Network information). Figure 3 shows one of the original gather, classified primary and multiple.

Multiple prediction and reservoir characterization of a tight sand reservoir

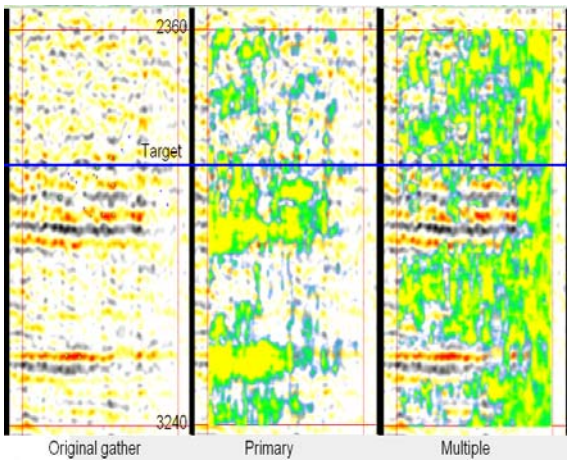

Figure 3. One of the original gather, classified primary, and multiple. The green dots on the original gather are picked primary locations; the blue dots are picked multiple locations. One gather has 100 traces. The red lines are the boundaries of the steering cube. The thick blue horizontal line is the target horizon.

After classification, we stack the primary and multiple possibilities into primary cube and multiple cube. Comparing the classified primary and the stack of raw gathers, we found that these two volumes were very similar. Therefore we draw a conclusion that most of the dipping multiples on raw gathers were attenuated by stacking.

In the post stack approach we apply the same kind of procedure, however with post-stack attributes. Attributes include variation of amplitude strength between partial offset stacks, variation of amplitude strength between azimuthal stacks, misalignment of events between partial offset stacks and misalignment of events between stacks and frequency content. The rational of this technique was that: if there is multiple energy interfering with an event we expect more misalignment and irregular amplitude variations between the different stacks. Also the frequency content might be lower due to interference with primaries. Subsequently we picked points in the volume that we assessed as having low, moderate and high multiple interference respectively. The classification is done by the user, based on the gather views. Subsequently a NN is trained to recognize the zone of low, moderate and high multiple contamination and applied to the whole reservoir area.

Multiple removal and thickness estimation

Also two methods for multiple elimination were applied: predictive deconvolution and radon based demultiple

We applied predictive deconvolution to see if we may get a better amplitude-thickness relationship. The predictive deconvolution used is Predictive Error Filter in Seismic Unix. We found that an operator length of 28 ms and a predictive length of 120 ms gave a better amplitude-thickness relationship. We also tried Radon transform with Hampson-Russell software. Figure 4 shows the amplitude-thickness relationship after predictive deconvolution and Radon transform.

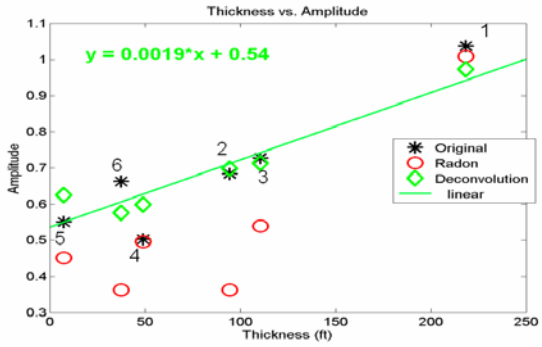

Figure 4. The relationship between amplitude and thickness after predictive deconvolution and Radon transform. All of the three amplitudes (original, after Radon, after decovolution) were normalized according to their surveys). The green line is the linear fit to deconvolution result. The function in green letters is the linear regression function of the green line.

We also observed that the primary after deconvolution had similar pattern with acoustic impedance inversion nearby well 6 (Figure 5). Where the Acoustic Impedance inversion was low in the small square in Figure 5, the primary after deconvolution was also low.

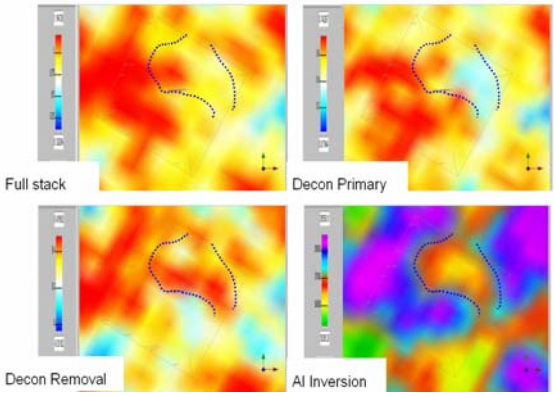

Figure 5. Map views of well 6 from full stack, primary and multiple after deconvolution, and acoustic impedance. The squares in the center of the four smaller figures are scales to indicate the inlines and crosslines which are five traces

Multiple prediction and reservoir characterization of a tight sand reservoir

away from well 6. Well 6 is centered in those squares. The dashed lines are digitized from the pattern of Acoustic Impedance inversion, and then are plotted on the other three figures. The primary after deconvolution has similar pattern with acoustic impedance inversion.

Multi-attribute analysis

To derive the best possible thickness estimation we combined peak amplitude and impedance in predicting thickness. Although both peak amplitude and impedance show relationships with thickness, neither of them could separate the thin and thick wells at the reservoir in our study. We considered a reservoir thickness above 80 feet as thick and economical. If a well has a thickness of 70 or less, we consider it as a thin well. Figure 6 shows the crossplot of peak amplitude and acoustic impedance. In the peak amplitude and acoustic impedance crossplot, the thick and thin wells are becoming separable.

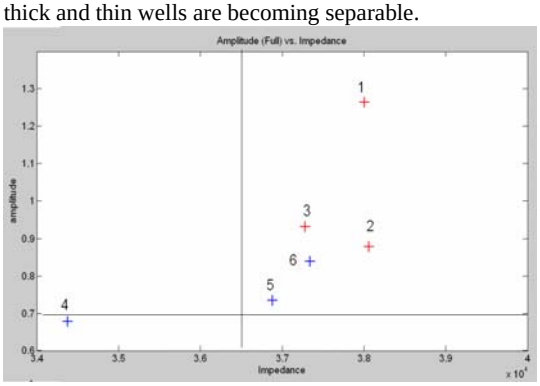

Figure 6. The crossplot of peak amplitude and acoustic impedance. The wells with thickness above 80 are plotted as red "+", and the wells with thickness below 80 are plotted as blue "+". The black lines are cutoff values.

We first applied cutoff values to make thin and thick classifications. In our dataset, if the impedance is below $3.5x10^4$, most likely it will be a thin well; if the peak amplitude is less than 0.7, most likely it will be a thick well. We applied Support Vector Machine (SVM) to separate thin and thick wells in the region where the peak amplitude and impedance were higher than cutoff values. An SVM is an algorithm using selected examples (known as support vectors) in classification. The theory of SVM was introduced to the computer learning community in the mid 1990s (Vapnik, 1995). The SVM application of seismic attributes classification can be found in Li and Castagna (2004), Zhao et al. (2005).

Figure 7 shows the map view of the multi-attribute classification results. Validation from the three withheld wells (not used in this study) shows that this method predicts two withheld wells into right category. It only misclassified one of the three withheld wells.

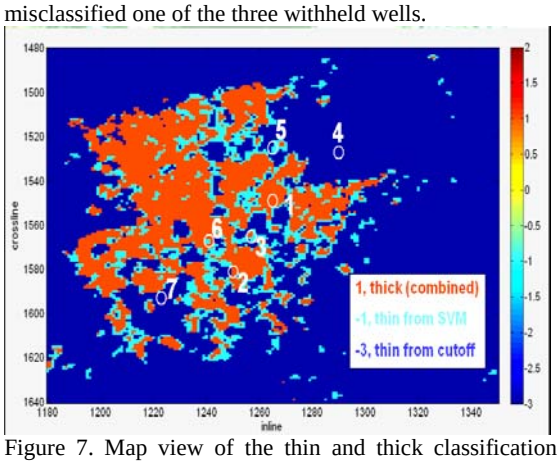

Figure 7. Map view of the thin and thick classification results. Dark blues (-3) stands for classified thin area according to cutoff values. Light blue (-1) stands for classified thin area according to Support Vector Machine. Red (1) stands for classified thick area from both cutoff values and Support Vector Machine.

Conclusions

From pattern recognition analysis, we found that multi attribute NN can highlight multiples pre-stack and post-stack. The similarity between classified primary from pre-stack pattern recognition and the stack of raw gathers indicated that most of the dipping multiples on raw gathers were attenuated by stacking. Although both Radon and deconvolution demultiple algorithms gave a better thickness-amplitude relationship for the available wells. However not all of the blind wells were predicted correctly. The multi-attribute analysis of acoustic impedance and peak amplitude is very effective in highlighting the economical reservoir.

Acknowledgements

We thank Anadarko Petroleum and WesternGeco for permission to show the seismic data. We thank David Connolly and Kristofer Tingdahl for their help and input for this project.

EDITED REFERENCES

Note: This reference list is a copy-edited version of the reference list submitted by the author. Reference lists for the 2008 SEG Technical Program Expanded Abstracts have been copy edited so that references provided with the online metadata for each paper will achieve a high degree of linking to cited sources that appear on the Web.

REFERENCES

Aminzadeh, F., and P. de Groot, 2005, A neural networks based seismic object detection technique: 75th Annual International Meeting, SEG, Expanded Abstracts, 775–778.

Li, J. K., and J. Castagna, 2004, Support vector machine (SVM) pattern recognition to AVO classification: Geophysical Research Letters, **31**, L02609, doi:10.1029/2003GL018299.

Vapnik, V. ,1995, The nature of statistical learning theory: Springer-Verlag.

Zhao, B., H. W. Zhou, and F. Hilterman, 2005, Fizz and gas separation with SVM classification: 75th Annual International Meeting, SEG, Expanded Abstracts, 297–300.